GA–A22902

METHOD OF NEUTRAL DENSITY DETERMINATION NEAR THE X–POINT IN DIII–D

by

R.J. COLCHIN, R. MAINGI, ME.E. FENSTERMACHER, T.N. CARLSTROM, R.C. ISLER, and L.W. OWEN

JULY 1998

DISCLAIMER

GA–A22902

METHOD OF NEUTRAL DENSITY DETERMINATION NEAR THE X–POINT IN DIII–D

by

R.J. COLCHIN,† R. MAINGI,† ME.E. FENSTERMACHER,‡ T.N. CARLSTROM, R.C. ISLER,† and L.W. OWEN†

This is a preprint of a paper to be presented at the 25th European Physical Society Conference on Controlled Fusion and Plasma Physics, June 29–July 3, 1998, Prague, Czech Republic, and to be published in the *Proceedings.*

†Oakridge National Laboratory

‡Lawrence Livermore National Laboratory

Work supported by
the U.S. Department of Energy
under Contracts DE-AC03-89ER51114, DE-AC05-96OR22464,
and W-7405-ENG-48

GA PROJECT 3466
JULY 1998

Method of Neutral Density Determination Near the X–Point in DIII–D*

R.J. Colchin,† R. Maingi,† M.E. Fenstermacher,‡ T.N. Carlstrom, R.C. Isler,† L.W. Owen†

General Atomics, P.O. Box 85608, San Diego, CA 92186-5608

A new method for determining the density of neutrals near the X–point of a diverted plasma is described. Code calculations have predicted that the neutral density peaks poloidally near the X–point [1] and there is evidence that neutrals play a role in the L–H transition [1–3] and in damping the plasma rotation [4]. The new method uses D_α data from a tangentially-viewing video camera calibrated by a vertically-viewing photomultiplier. These data, combined with electron temperature and density measurements from the divertor Thomson scattering (DTS) system, provide sufficient information to determine the neutral density in the X–point region of DIII–D. Preliminary results show neutral densities above the X–point are of order 10^{10}–10^{11} atoms/cm^3. The diagnostics used to determine these neutral densities, the data analysis method, and preliminary results are described in this paper.

Diagnostics

The technique used to determine the neutral density employs the 2D image of D_α light from a tangentially-viewing video camera [5], referred to as the tangential TV (TTV). Light from the divertor region is imaged onto a fiber optic bundle via a stainless steel mirror-and-lens system. Light from the fiber optic bundle is parallelized, split into two beams, passed through two D_α notch filters, and imaged onto two charge-induction video cameras, one of which has a four-times higher gain. The mirror views the divertor at about the height of the X–point of a typical lower-single-null equilibrium, and enables the cameras to view the whole divertor region from the inner wall to the outside ring and baffle structure. The optical system has a large depth of field, and so views ~90° in toroidal angle.

The cameras frame at the standard video rate of 30 full-interlaced frames/s or 60 half-interlaced frames (256 vertical by 512 horizontal pixels) per second. Using half frames, it is possible to obtain an image every 17 ms. Video data is stored on high-quality magnetic tape and selected data is later digitized. Because the cameras view ~90° toroidally, a reconstruction algorithm [5] must be used to obtain profiles in a poloidal plane. To perform the reconstruction, toroidal symmetry is assumed and each pixel is treated as a chordal measurement. The reconstruction is accomplished via a matrix equation $\vec{A}M = \vec{B}$, where $\vec{A}$ is the 2D solution in a poloidal plane and $\vec{B}$ is the raw data. To restrict the translation matrix M to manageable size, the data is resampled to 128×128 and the solution image has a 2 cm ($50 \times 3\ 0$ grid) spatial resolution. The matrix equation is solved using least squares regression techniques. The area of the reconstructed solution is shown in Fig. 1.

The TTV system is not absolutely calibrated. Cross-calibration is provided by an array of seven photomultiplier detectors which vertically view D_α light in the lower divertor. Plasma light is imaged onto optical fibers and passed through D_α notch filters in the same manner as

*Work support by U.S. Department of Energy under Contracts DE-AC03-89ER51114, DE-AC05-96OR22464, W-7405-ENG-48.

†Oak Ridge National Laboratory, Oak Ridge, TN, USA.

‡Lawrence Livermore National Laboratory, Livermore, CA, USA.

the TTV. This arrangement is called the Filterscope (FS). The FS chord nearest to the data points of the DTS, which is the chord used in these measurements, is shown in Fig. 1. D_α data is also available from a similar set of vertical chords viewed by the multichord divertor spectrometer (MDS). Both the MDS and FS diagnostics have been calibrated by an integrating sphere light source (Oprtonics Laboratory, Unisource 6000) in photons/cm^2-s-steradian. The location of the chords and the divergence of their light cones were determined by back-lighting the optical fibers. Calculations indicate that only ~5% of the light viewed by the FS chord shown in Fig. 1 comes from outside the area viewed by the TTV.

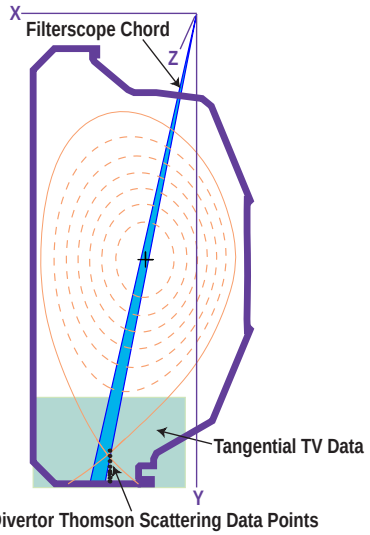

Fig. 1. DIII–D vacuum chamber cross section showing the filterscope chord, DTS measurement locations, coordinates used in the TTV-FS calibration, and the area into which the TTV data is reconstructed. The flux surfaces shown apply to the equilibrium with the 17.5 cm high X–point.

Calibration of the TTV Intensity

To measure neutral densities, it is necessary to absolutely calibrate the TTV via the FS or MDS. The FS and MDS view the plasma approximately within a cone, while the TTV data is projected onto a poloidal cross section. Data from the TTV within the boundary of a FS and MDS cone is integrated and compared with the FS or MDS signal intensity. In the following discussion, while the FS geometry is assumed, the same calibration procedures apply to the MDS.

The coordinate system used in the TTV-FS data normalization is shown in Fig. 1. The assumption of toroidal symmetry implies constancy of the TTV data in the *z* direction (i.e. toroidal effects are ignored since the radius of the FS cone is small compared to the major radius of the TTV data). The neutral density is given by

$$n_o(y) = S_{tot}(y)\frac{4\pi S_{FS}\overline{A}}{R_y S_{tot}} \qquad (1)$$

where S_{tot} is the integrated TTV signal within the FS cone, $S_{tot}(y)$ is the TTV signal within the FS cone at height *y*, S_{FS} is the FS signal, $\overline{A}$ is the TTV signal-weighted average area of an *x*-*z* cross section of the Filterscope's cone, and R_y is the D_α excitation rate coefficient at height *y*.

The D_α light intensity is linked to the neutral density through electron excitation rate coefficients [6] which are sensitive functions of the electron density and temperature, particularly at temperatures below 10 eV. For electron temperatures above ~1.5 eV, electron ionization of neutrals dominates over recombination. A plot of the excitation coefficients $\langle \sigma_{exc} v \rangle = R_y / n_e$ is shown in Fig. 2. Code calculations indicate that the plasma should be optically thin to D_α radiation [7]. The density and temperature are measured by the DTS [8]. Measurement locations are shown in Fig. 1.

Preliminary Results

A series of discharges were run in DIII–D in L–mode, just below the H–mode power threshold. For the data shown, the line average density was 2.5×10^{19} m^{-3}, I_p = 1 MA, B_T =

2.1 T, P_{ohmic} = 0.83 MW, $\langle P_{BEAMS} \rangle$ = 0.25 MW, and the ∇B drift direction was downward. The equilibrium was adjusted so that two or three DTS data points were at or above the X–point (Fig. 1) when the X–point was at the same major radius as the DTS.

Preliminary data were taken from two discharges with the X–point located at the radial position of the DTS for 0.5 s. In one discharge the X–point was positioned 12.5 cm above the divertor floor and in the other discharge it was 17.5 cm above the floor. DTS electron temperatures and densities were recorded at 50 ms intervals during the half-second that the X–point was at the DTS location, and were combined to give average values. Figure 3 shows the results for the higher X–point discharge. Also shown is the normalized intensity of the TTV data, integrated across the ~10 cm diameter of the FS cone. Line average densities for these discharges were 2.5×10^{19} m^{-3}.

The neutral densities for the two previously-discussed discharges are shown in Fig. 4. Neutral densities for the lower (12.5 cm) X–point discharge are shown as dots, and were derived from a single TTV frame. Data for the 17.5 cm X–point, shown as squares, were averaged from seven TTV frames.

There are several sources of possible error in these measurements. The TTV data has ripples resulting from the method of least squares analysis used in solving the reconstruction matrix and the low signal-to-noise levels present in these experiments.

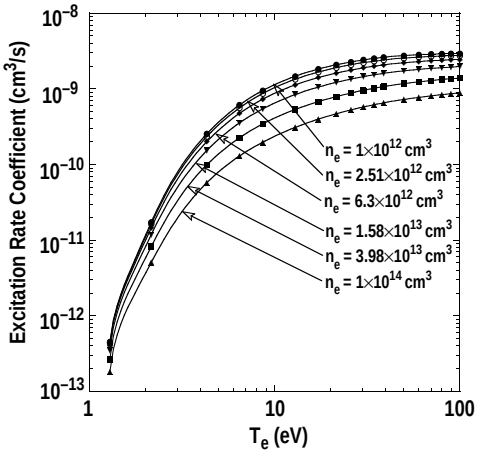

Fig. 2. Electron excitation rate coefficients $\langle \sigma_{exc} v \rangle = R_{i_y}/n_e$ *as a function of the electron density and temperature.*

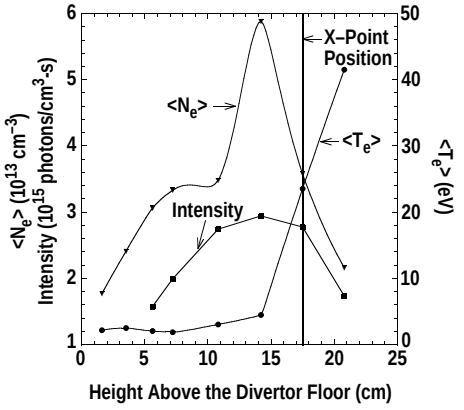

Fig. 3. Electron temperatures and densities as determined by the DTS and averaged over 10 time points during the discharge with the X–point at a height of 17.5 cm. Also shown is the intensity of the TTV integrated over a 2 cm high slice through the FS light cone.

We have smoothed the data to eliminate these ripples, and in future work we will attempt to eliminate this source of error. However as seen in Fig. 3, there is not a large variation in the TTV intensity data. The TTV noise limit is ~5×10^{14} photons/m^3 indicating signal-to-noise levels of 2–10. The data variation of the FS calibration signal over the seven frames of the higher X–point data was 14.5%. By far the largest variations result from fluctuations in the DTS temperatures and densities. This is because of the steep fall off in the electron excitation coefficients shown in Fig. 2 at temperatures below 10 eV.

To assess the effect of these variations on the neutral densities, neutral density determinations were made for each of the seven TTV individual frames using the DTS data taken at the time of the frame. Figure 4 shows the resulting spread in data as error bars. The variations are smallest inside the X–point (i.e., at the points farthest above the divertor floor) where the electron temperatures are above 12 eV and the excitation coefficients are not a strong function of temperature. Below the X–point the electron temperatures are below 6.5 eV and the spread in the data becomes much larger.

The neutral densities shown in Fig. 4 represent an average of the TTV intensities integrated over a 2 cm high slice through the FS light cone, (Fig. 1) and must be interpreted over this volume. This spatial resolution can be improved if higher signal-to-noise TTV signals can be achieved. There is considerable attenuation of the neutrals in the private flux region (below the X–point) which is a consequence of the electron densities of ~1.8–6 × 10^{19} m^{-3} and temperatures of ~2–6 eV recorded by the DTS diagnostic. Preliminary results show that the neutral densities near the X–point are ~10^{11} atoms/cm^3 for both X–point heights, and in the range 10^{10}–10^{11} atoms/cm^3 above the X–point.

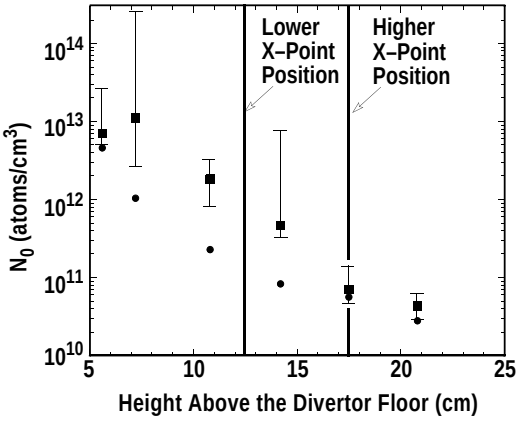

Fig. 4. Preliminary neutral densities as a function of height above the divertor floor. Neutral densities for a discharge with an X–point at 12.5 cm are shown by dots and data for a second discharge with a 17.5 cm X–point are shown by squares. Data for the higher X–point cases are the sum over ten DTS points and seven TTV frames. Error bars show the maximum data spread determined by calculating the data for each of the seven frames.

References

[1] B.A. Carreras, *et al.*, "Effect of Edge Neutrals on the Low-to-High Confinement Transition Threshold in the DIII–D Tokamak," to be published in Phys. of Plasmas.

[2] T. Fukuda, e*t. al.*, Proc. 16th IAEA Fusion Energy. Conf., Montreal, Canada, Vol. 1, p. 875 (International Atomic Energy Agency, Vienna, 1997).

[3] H.J. de Blank, J. Stober, and W. Suttrop, Proc. 23rd EPS Conf. on Contr. Fusion and Plasma Phys., Kiev, Vol. 20C, Part I, p. 99.

[4] P. Monier-Garbet, *et al.*, Nucl. Fusion **37** (1997) 403.

[5] M.E. Fenstermacher, *et al.*, Rev. Sci. Instrum. **68** (1997) 974.

[6] R.K. Janev and J.J. Smith, *Atomic and Plasma-Material Interaction Data for Fusion*, Supplement to the J. Nucl. Fusion (International Atomic Energy Agency, Vienna, 1993), Vol. 4, p. 1.

[7] H. A. Scott, *et al.*, "Impact of Detailed Radiation Transport on Volume Recombination," submitted to J. Nucl. Mater.

[8] D.G. Nilson, *et al.*, Fusion Eng. & Design **34-35** (1997) 609.